

Urban Heat Island Index Change Detection Based on Land Surface Temperature, Normalized Difference Vegetation Index, Normalized Difference Built-Up Index: A Case Study

Mas'uddin¹, Lina Karlinasari^{1,2*}, Setyo Pertiwi³, Erizal⁴

¹ Natural Resources and Environmental Management Science Study Program, Graduate School, IPB University, Baranangsiang Campus, Bogor 16144, Indonesia

² Department of Forest Products Technology, Faculty of Forestry and Environment, IPB University, Darmaga Campus, Bogor 16113, Indonesia

³ Department of Mechanical and Biosystem Engineering, Faculty of Agricultural Technology, IPB University, Darmaga Campus, Bogor 16113, Indonesia

⁴ Department of Civil and Environmental Engineering, Faculty of Agricultural Technology, IPB University, Darmaga Campus, Bogor 16113, Indonesia

* Corresponding author's e-mail: karlinasari@apps.ipb.ac.id

ABSTRACT

Climate change is a matter of considerable global importance, as evidenced by the increased urban surface temperatures in developed and undeveloped areas. Hence, this study aims to analyze the threshold and index of the urban heat island (UHI) phenomenon within the urban region of Bima City, located in Indonesia. The study was undertaken by utilizing sequential data from 2016, 2019, and 2022 obtained from the Google Earth Engine portal. The analysis focused on the assessment of UHI by examining land surface temperature (LST), normalized difference vegetation index (NDVI), and normalized difference built-up index (NDBI). Algorithms that operate on a single channel are employed to compute the land surface temperature. The findings indicate that the LST peaked in 2016 at 32.54 which rose to 35.08 in 2019 and increased to 39.18 in 2022. This implies a progressive rise in the LST of Bima City as time progresses. Moreover, it was observed that LST exhibited a positive correlation with the NDBI while displaying a negative correlation with the NDVI. The urban heat island phenomenon has been observed to possess the capacity to elevate ambient air temperatures in urban regions by as much as 3 when compared to suburban areas. In addition to considering both developed and undeveloped regions, it is important to acknowledge the observed changes in the UHI threshold in Bima City. Specifically, the UHI threshold has exhibited an upward trend, rising from 26.73 in 2016 to 29.57 in 2019 and 31.21 in 2022.

Keywords: climate change, geographic information system, urban heat island threshold.

INTRODUCTION

Climate change is a matter of utmost global importance, encompassing the phenomena of global warming and the escalating impact of greenhouse gases. The rise in temperatures and alterations in weather patterns have been observed (EEA, 2017). According to the World Health Organization Regional Office for Europe (WHO, 2017), more severe heatwaves, fires, and floods are growing, as well as an elevated prevalence of food and water-borne diseases. The United

Nations Environment Programme (UNEP, 2022) has reported that the building and urban construction sector is responsible for 37% of global greenhouse gas emissions and 34% of energy consumption. According to Nuruzzaman (2015), the utilization of construction materials and structures that are not environmentally friendly can result in the reflection and re-emission of solar radiation, leading to elevated surface temperatures in urban regions. The phenomenon commonly referred to as urban heat islands (UHI), where in urban centres exhibit higher surface temperatures

compared to suburbs or rural areas, has garnered significant attention due to its purported role in contributing to global warming and the amplification of greenhouse gas effects (Condo et al. 2021) cooling behaviours are increasingly important for city dwellers. Cooling actions, especially air conditioning, receive increasing scrutiny in social science, as does engagement and communication on behaviours spanning adaptation and mitigation. In response, this paper evaluates the relation between residents' adaptation and mitigation behaviours around cooling in Fukuoka, Japan, and draws lessons for communication on encouraging adaptation and mitigation actions. A survey distributed to residents in six areas of Fukuoka, Japan, assessed perceptions of global warming and urban heat island effects, frequency of mitigation and adaptation behaviours, use of air conditioning, electricity bills and evaluation of green spaces. We observe a difference between respondents using air conditioning with an energy-saving (i.e. mitigation).

Urbanization in cities has exerted significant influence on the allocation of land use and the composition of urban land cover, which is increasingly dedicated to development endeavours such as industrialization, road infrastructure, and the construction of buildings using materials with high thermal capacity. The study by Kamboj and Ali (2020) focuses on developing a hydrophobic surface and its ability to absorb solar radiation efficiently. Human activities have the potential to alter the natural environment, thereby disrupting the impact of natural conditioning (Ahmed 2018). In addition to substantial human-induced alterations of urban land surfaces, the geospatial distribution of these modifications can amplify the impacts of heat waves (Athukorala and Murayama 2021). According to the research conducted by Tawfeeq Najah et al. (2023), the factors that need to be considered concerning building height include formation and ground cover. The potential for developing UHI has been identified (Alavipanah et al. 2018).

The phenomenon of urban heat islands has been observed in various cities in Indonesia, including two big cities of Yogyakarta (Fawzi 2017) and Semarang (True et al. 2019). Extensive research has been conducted, revealing conditions already of significant concern. The conditions in Yogyakarta exhibit a phenomenon known as urban sprawl, wherein the city's physical expansion exceeds its administrative boundaries. This

expansion has led to an increased intensity of the UHI effect, which influences the temperature of the city and its surrounding areas. According to Khoshnoodmotlagh et al. (2021), urban expansion and the resulting alteration of natural land cover contribute to the intensification of local climate change.

Based on the presented case, the potential conversion of vegetated lands into developed areas due to urban development and urbanization patterns may catalyze the manifestation of urban heat island phenomena in various cities, including Bima City, West Nusa Tenggara Province. The population data of Bima City in 2016 was reported to be 138,287 individuals (DKPS 2016). In 2022, the population is projected to reach 157,851 individuals (DKPS 2022), indicating a significant increase of 13.84% during the specified period. Setiawan and Rudiarto (2016), Ismoyojati et al. (2019), and Nisah (2022) have provided explanations regarding the dynamic nature of land use activities in Bima City between the years 1996 and 2021, highlighting the annual changes that have occurred.

The conversion of land for vegetation experienced a decrease of 2918.4 hectares, while the conversion of land for rice fields decreased by 407.4 ha. The quantity of developed, undeveloped, and bodies of water progressively expands annually. According to Nisah (2022), there was a notable increase in built-up land, open land, and ponds in Bima City. Specifically, built-up land expanded by 1331 ha, open land by 1177.4 ha, and ponds by 42.3 ha. This growth in various land types has contributed to the overall expansion of critical land in Bima City. Garouani et al. (2021) have established that alterations in land cover utilization exert substantial effects on climate by influencing surface temperature and precipitation through multiple mechanisms the occurrence of heavy precipitation and changes in the upstream watershed conditions, specifically a decrease in area. As mentioned above, the decrease resulted in a subsequent expansion of urbanized areas within Bima City. In the year 2016, a catastrophic flood occurred. The main causative factor in the occurrence of a major flood disaster is suspected. Ismoyojati et al. (2019) have observed that land use changes substantially influence the alterations in watershed responses to precipitation events.

Based on the available data, there exists a suspicion regarding the potential occurrence of the urban heat island phenomenon in Bima City.

Consequently, it is imperative to identify, analyze, and assess the presence of the UHI phenomenon in Bima City. A thorough comprehension of the spatial-temporal variations of a region and the phenomenon known as the urban heat island is crucial for policymakers to develop sustainable development strategies (Yang et al. 2020). Hence, this investigation aims to analyze the urban heat island threshold and index within the urban region of Bima City, Indonesia, during the years 2016, 2019, and 2022.

MATERIALS AND METHODS

The focus of this study was the entire area of Bima City, West Nusa Tenggara Province, Indonesia. Bima City encompasses an area of 20 805 ha. Geographically, the city is located at 118°411' – 118°481' East Longitude and 8°201' – 8°301' South Latitude as indicated in Figure 1. It is bordered on the north by Ambalawi District, on the east by Wawo District, on the south by Belo District, all in Bima Regency, and on the west by Bima Bay.

Examination and interpretation of data

The process of examining and interpreting data. Subsequently, the gathered data is subjected to remote sensing methodologies for processing.

The present study utilizes Landsat 8 OLI/TIR imagery acquired in 2016, 2019 and 2022 from the United States Geological Survey (USGS). The research site is situated in Bima City. Research data processing is conducted by utilizing a Geographic Information System (GIS) methodology and incorporates remote sensing techniques.

Identification process

In order to ascertain the spatial patterns of urban heat islands, it is imperative to discern the land surface temperature (LST). The process of identification can be divided into the following stages:

1) Identification of temperature brightness. The data analysis process uses LST algorithms formulated using temperature brightness techniques described in the following steps:

- Digital Number to Spectral Radian. The first thing to do is convert the digital numbers on Landsat 8 into spectral beams using the following equation (Ultrasound 2019).

$$L_{\lambda} = M_L \cdot Q_{cal} + A_L \quad (1)$$

where: L_{λ} – spectral radians, M_L – scale factor, Q_{cal} – digital number, A_L – adding factor.

- Convert Radians into Kelvin. The need to convert the value of radians into kelvins and then convert them into Celsius units is to make it easier for people to read them, and

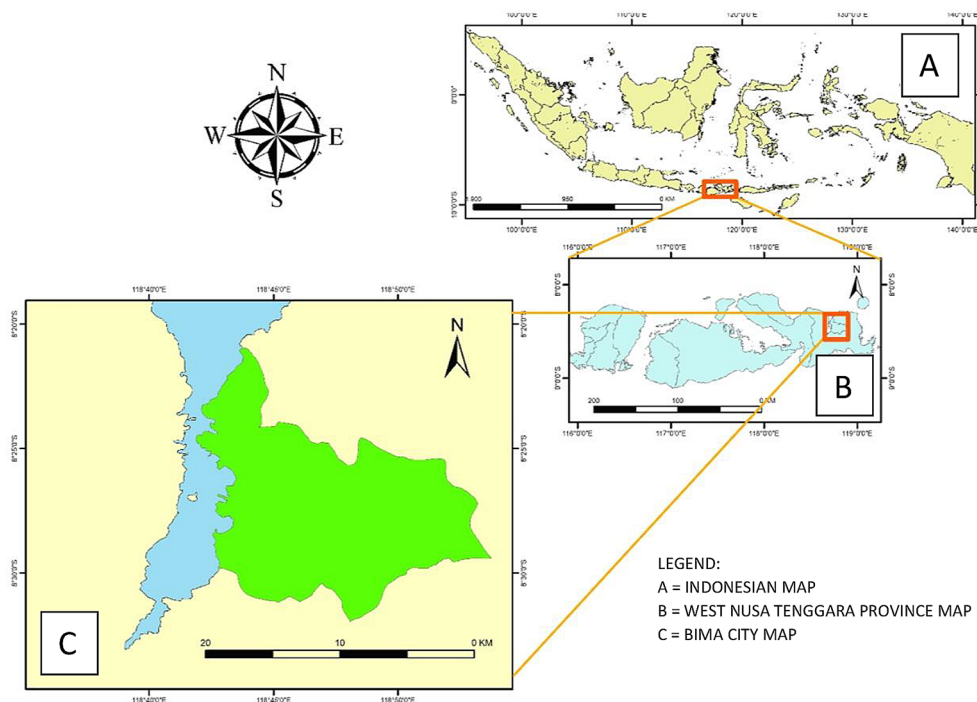


Figure 1. Study location

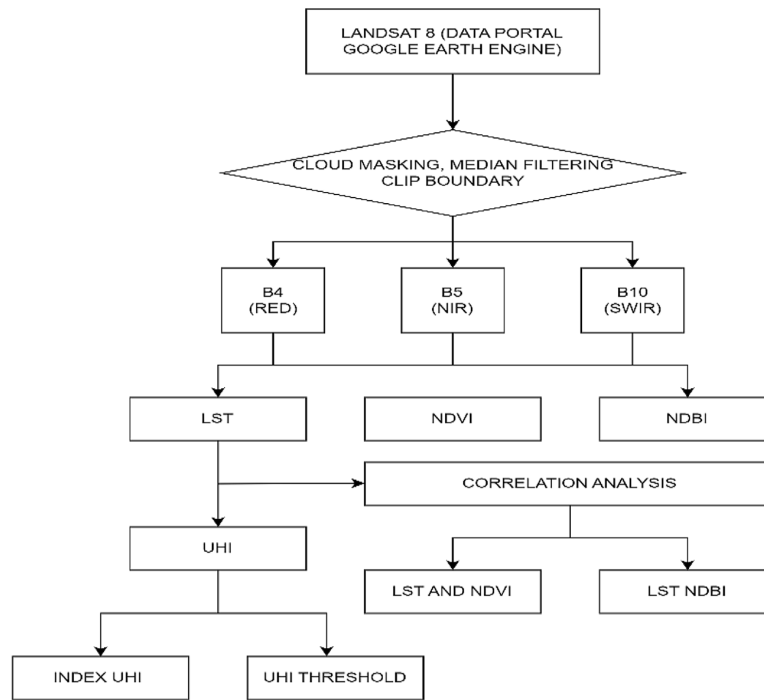


Figure 2. Flow chart of research study

will be described in the following formula (USGS 2019):

$$T = K_2 / \ln(K_1 / L_\lambda + 1) \quad (2)$$

where: T – temperature (K), L_λ – radian value in the thermal band, K_1 – spectral radian calibration constant ($W/(m^2 \cdot sr \cdot \mu m)$), K_2 – absolute temperature calibration constant (K).

- Convert Kelvin value into Celsius. To convert the kelvin value into Celsius using the following formula (USGS 2019):

$$B_T = T - 273.15 \quad (3)$$

where: B_T – temperature brightness, T – temperature (K).

- Looking for the normalized difference vegetation index (NDVI). NDVI is a method for finding vegetation values. In finding the NDVI soil surface temperature is useful to determine the emissivity found in the area studied, the NDVI formula will be described as follows (Akher and Chattopadhyay 2017):

$$NDVI = \frac{NIR - RED}{NIR + RED} \quad (4)$$

where: NIR – near infrared radiation from pixels, RED – red light radiation from pixels.

- Find the value of proportion of vegetation (PV). To obtain PV values, it is necessary to scale NDVI to minimize interference from

moist soil conditions and surface energy flux. The PV value is obtained by the following equation (Akher and Chattopadhyay 2017):

$$PV = \frac{[(NDVI - NDVI_{min})]}{(NDVI_{max} + NDVI_{min})} \quad (5)$$

where: $NDVI_{min}$ – smallest value, $NDVI_{max}$ – highest value.

- Determine the normalized difference built-up index (NDBI). NDBI is an algorithmic method that involves middle infrared and near infrared waves with a band 10 and 5 each. Spectral range also between 0.1 and 0.3 (Kaplan et al. 2018). The equation used to determine NDBI is presented as follows:

$$NDBI = \frac{SWIR - NIR}{SWIR + NIR} \quad (6)$$

where: SWIR – band with a middle infrared wavelength, NIR – band with a near infrared wavelength.

- Land surface emissivity. Surface emissivity is especially important to reduce errors in estimating surface temperatures using satellite imagery. Several methods were developed to derive surface emissivity from remote sensing data. One easy alternative to obtain surface emissivity is to use the processed vegetation index to obtain PV values with the following equation (USGS 2019):

$$E = 0.0004 \cdot PV + 0.986 \quad (7)$$

where: 0.004 – average emissivity value of vegetation categorized as dense, 0.986 – standard emissivity value of open land

- Land surface temperature (LST) (Jimenez-Munoz et al. 2014). After knowing the emissivity value and changing the digital number value into radiance and changing the kelvin temperature to Celsius, then LST can be formulated and determined. using the following equation:

$$LST = \left(\frac{BT}{1+W} \times \frac{BT}{1+p} \right) \times 1n(E) \quad (8)$$

where: BT – satellite brightness temperature (°C),
W – radiation wavelength (11.5 μm),

$$p = h \cdot c / s \quad (14380 \text{ mK}),$$

$$h - \text{Planck's constant} - 6.626 \cdot 10^{-34} \text{ Js},$$

$$c - \text{speed of light} - 2.998 \cdot 10^8 \text{ m/s},$$

$$s - \text{Boltzmann's constant} - 1.38 \cdot 10^{-23} \text{ J/K},$$

$$E - \text{surface emissivity}$$

2) Urban heat island analysis

Urban heat islands (UHI) were determined using LST obtained from previous analyses. The stages analyses were as followed:

- Set a threshold for the lowest surface temperature that qualifies as an urban heat island. The value is set at 3 °C based on expert opinion.
- Determine the UHI threshold to represent the temperature value at which the urban heat island phenomenon is observed using the following equation (Kaplan et al. 2018).

$$UHI = \mu + \frac{\sigma}{2} \quad (9)$$

$$LST > \mu + \frac{1}{2}\sigma \quad (10)$$

Regions focus only on regions of the UHI phenomenon, whereas non-UHI regions can only occur during the following relationships (El-Hattab et al. 2018):

$$0 < LST \leq \mu + 0.5\sigma \quad (11)$$

- Calculates the UHI (Map) index using the following formula (Fawzi 2017):

$$UHI_{index} = T_{mean} - \left(\mu + \sigma \frac{1}{2} \right) \quad (12)$$

where: μ – the average surface temperature of the LST values obtained, σ – standard deviation of surface temperature based on the LST values obtained, T_{mean} – the median value of the LST class obtained.

RESULTS AND DISCUSSION

Determination of LST, NDVI, and NDBI in Bima City 2016, 2019 and 2022

In 2016, the highest recorded land surface temperature distribution in Bima City was 32.54 °C, covering an estimated 1,991 ha or 9.57% of the total area. Conversely, the lowest LST distribution was observed to be 20.50 °C, encompassing an area of 2,545 ha or 12.23% of the total area. These findings are presented in Table 1 and Figure 3. The findings indicate that the lowest recorded land surface temperature in 2019 was 20.72 °C, whereas the highest recorded LST was 35.08 °C. The average LST for the year was calculated to be 28.35 °C, with a standard deviation of 2.44 °C.

The analysis of NDVI values in 2016 revealed a range of values, with the minimum value recorded as -0.12, covering an area of 298.60 ha or 1.44% of the total area. On the other hand, the maximum value observed was 0.59, as depicted in Table 2 and Figure 3. Furthermore, the NDBI map illustrates that the lowest recorded value is -0.63, signifying the presence of a vegetated built-up area. Conversely, the highest recorded value of 0.47 is observed on land designated as built-up. Table 3 displays the temporal variations in the normalized difference built-up index. The data indicates that the largest NDBI area 2016 measured 1,960 ha, accounting for 9.42% of the total area. By 2022, this value had risen to 2,672 ha, representing 12.85% of the total area.

The LST value experienced a significant increase of 35.08 from 2016 to 2019. Additionally, the LST area expanded from 1,991 ha, accounting for 9.57% in 2016, to 3,517 ha, representing 16.91% in 2019.

The NDVI maximum value exhibited a decline from 0.59 to 0.54. It is anticipated that the LST values will experience a rise of 2.54 °C in 2019. In 2019, the highest recorded temperature reached 35.08 °C; in 2016, the maximum temperature observed was 32.54 °C. Therefore, indicating a positive trajectory. Furthermore, the NDVI exhibited values between -0.09 and 0.57, indicating a high level of greening during 2022. This greening was observed over 3,597 ha, accounting for approximately 17.3% of the total area under consideration. However, it is worth noting that this greening area experienced a reduction of 2,791 ha between 2016 and 2022, as illustrated in Table 2.

Table 1. The changes in LST Area for Bima City in 2016, 2019 and 2022

Class land surface temperature (°C)			Area (ha)						Changes in land surface temperature area			
									2016-2019		2019-2022	
2016	2019	2022	2016	%	2019	%	2022	%	Δ	Δ%	Δ	Δ%
20.50–23.38	20.72–24.55	16.99–24.82	2,545	12.23	1,639	7.89	1,665	8.00	- 906	- 4.35	25	0.12
23.38–25.13	24.5–27.08	24.82–27.78	5,088	24.45	3,821	18.38	3,115	14.97	- 1,267	- 6.08	- 706	- 3.40
25.13–26.64	27.08–28.88	27.78–30.13	6,522	31.34	5,921	28.48	5,515	26.51	- 600	- 2.87	- 407	- 1.97
26.64–28.39	28.88–30.68	30.13–32.31	4,659	22.40	5,895	28.35	6,424	30.88	1235	5.95	529	2.53
28.39–32.54	30.68–35.08	32.31–39.18	1,991	9.57	3,517	16.91	4,086	19.64	1,525	7.34	569	2.73
			20,805	100.00	20,805	100.00	20,805	100.00				

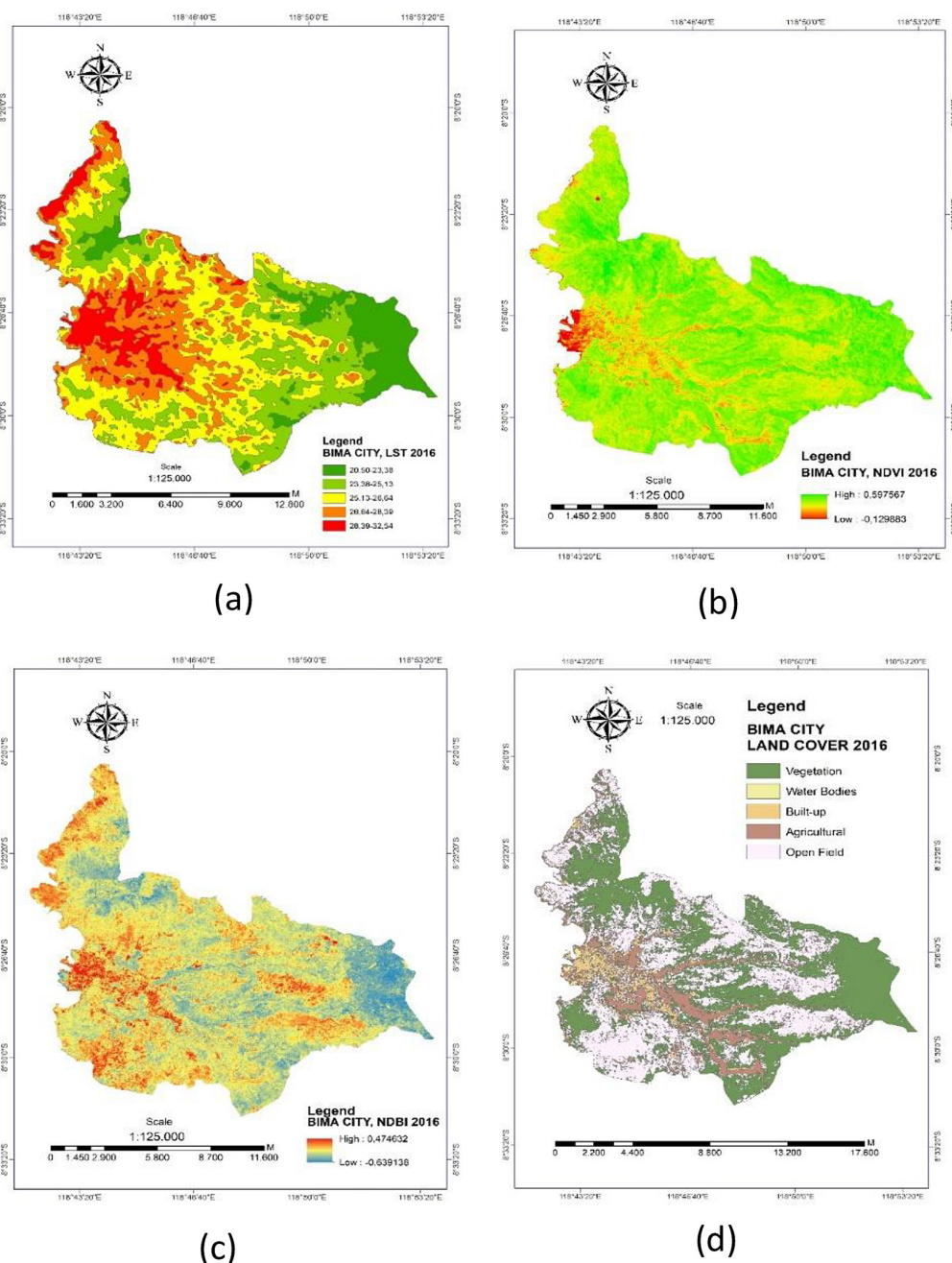


Figure 3. The results of LST (a), NDVI (b), NDBI (c) and land cover (d) for 2016

Table 2. The changes in area of NDVI density

Vegetation density	Area (ha)						NDVI area change			
	2016		2019		2022		2016–2019		2019–2022	
	2016	%	2019	%	2022	%	Δ	Δ%	Δ	Δ%
Land not vegetated	298	1.44	607	2.92	3,393	16.32	309	1.49	2,785	13.40
Very low greenness	1,810	8.71	3,885	18.69	5,413	26.04	2,074	9.98	1,528	7.35
Low green	4,715	22.68	6,731	32.38	4,216	20.28	2,016	9.70	-2,515	-12.09
Medium green	7,577	36.44	5,994	28.84	4,167	20.05	-1,582	-7.61	-1,828	-8.79
High greenery	6,388	30.73	3,570	17.17	3,597	17.30	-2,818	-13.56	27	0.13
Total	20,805	100.00	20,805	100.00	20,805	100.00				

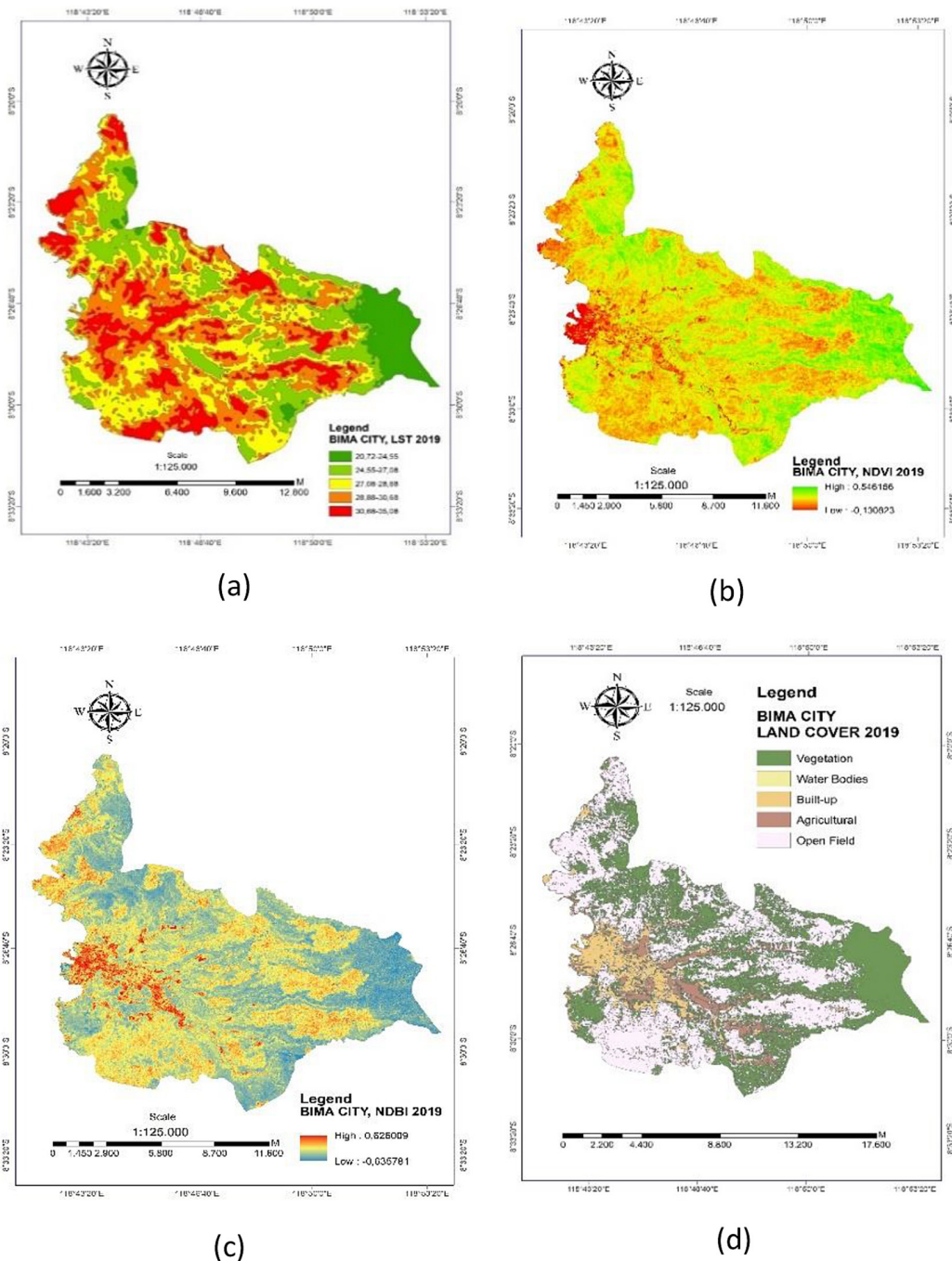


Figure 4. The results of LST (a), NDVI (b), NDBI (c) and land cover (d) for 2019

Table 3. The changes in NDBI area for Bima City in 2016, 2019 and 2022

Building density	Area (ha)						Changes in building density area			
	2016		2019		2022		2016–2019		2019–2022	
	2016	%	2019	%	2022	%	Δ	Δ%	Δ	Δ%
Non building	2,791	13.42	4,661	22.42	2,163	10.40	1871	9.00	- 2,498	- 12.01
Very low	5,715	27.47	6,180	29.72	4,369	21.01	465	2.25	-1,811	- 8.71
Low	6,229	29.94	5,108	24.56	5,474	26.33	- 1,122	- 5.38	366.65	1.76
Currently	4,109	19.75	3,845	18.49	6,114	29.40	- 264	- 1.26	2,269	10.91
High	1,960	9.42	999	4.81	2,672	12.85	- 961	-4.62	1,674	8.05
Total	20,805	100.00	20,805	100.00	20,805	100.00				

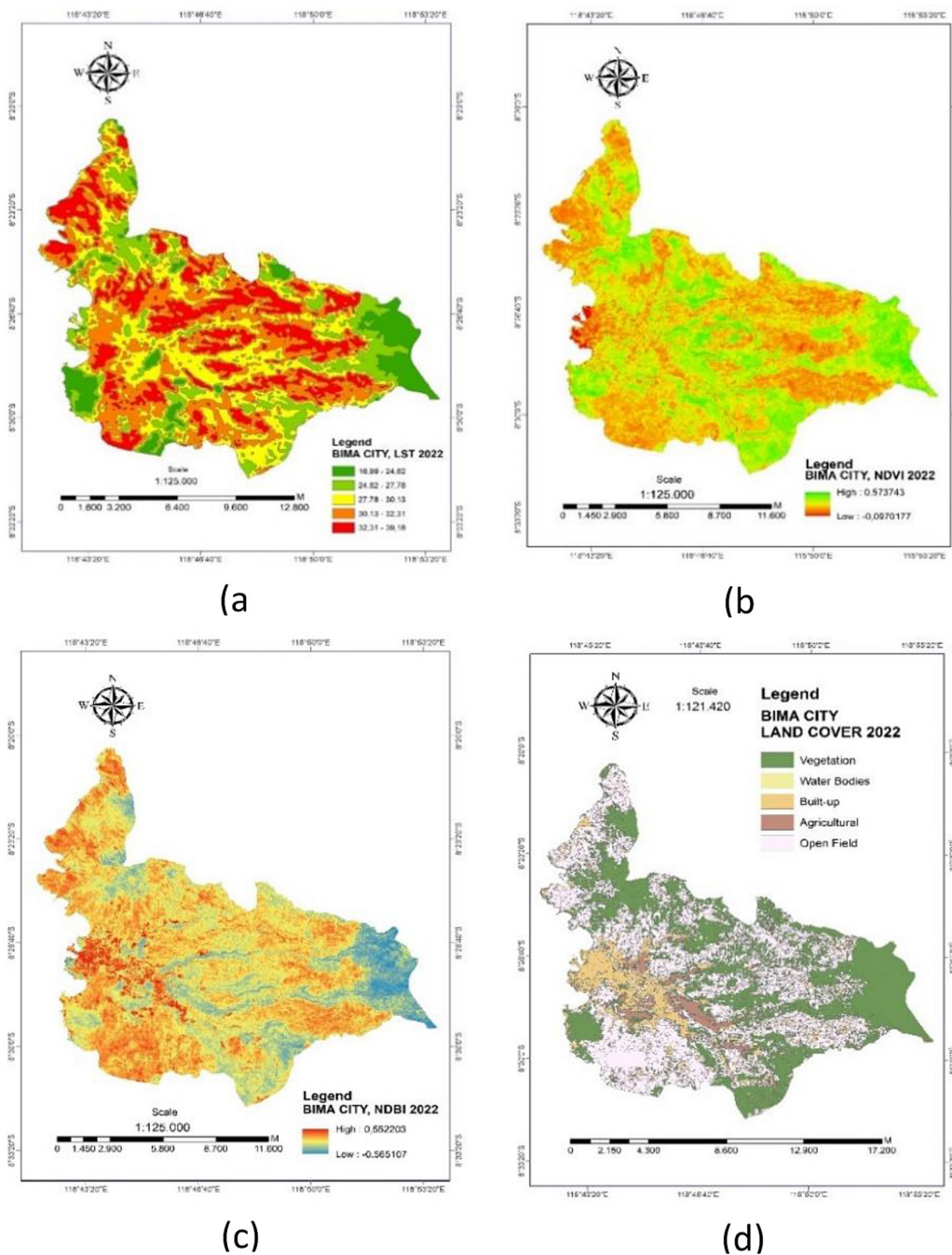


Figure 5. The results of LST (a), NDVI (b), NDBI (c) and land cover (d) for 2022

In 2022, the observed Land Surface Temperature (LST) values ranged from 16.99 to 39.18 . These values were recorded over 4,086 ha, which accounts for 19.64% of the total area. This information is visually represented in Figure 5 and quantitatively summarized in Table 1.

The relationship between LST and Normalized Difference Vegetation Index (NDVI) exhibits a robust negative correlation, indicating that a decrease in NDVI is associated with increased LST. The data reveals a notable decline in the extent of dense vegetation land, encompassing an area of 6,388 ha in 2016, but has since diminished to 3,957 ha as of 2022. In 2022, the density value was recorded as 0.57, whereas Table 1 demonstrates an increase in the maximum LST area. In 2022, the Normalized Difference Built-up Index (NDBI) analysis revealed values ranging from -0.56 to 0.55. This assessment encompassed an area of 4,497 ha, which constituted approximately 21.63% of the overall study area. Moreover, there is an observed positive correlation between LST and NDBI.

Relationship between LST, NDVI and NDBI

The association between LST and the two variables, NDVI and NDBI is elucidated through the utilization of correlation graphs. The findings indicated a robust inverse relationship between LST and NDVI between 2019 and 2022. This implies that an elevation in LST corresponded to a decline in the NDVI. Conversely, a decrease in LST was associated with an increase in NDVI. In 2016, the LST exhibited a range of values between 20 and 32, encompassing a spatial extent of 1.991 ha.

This area constituted 9.57% of the total land area under consideration. Concurrently, the NDVI values spanned from -0.12 to 0.44, covering a larger area of 6.388 ha, which accounted for 30.73% of the total land area. Notably, a moderate correlation between LST and NDVI can be observed in Figure 6.

The tables provided Tables 1, 2, and 3 display the variations observed in LST, NDVI, and NDBI during the year 2016. The study revealed a

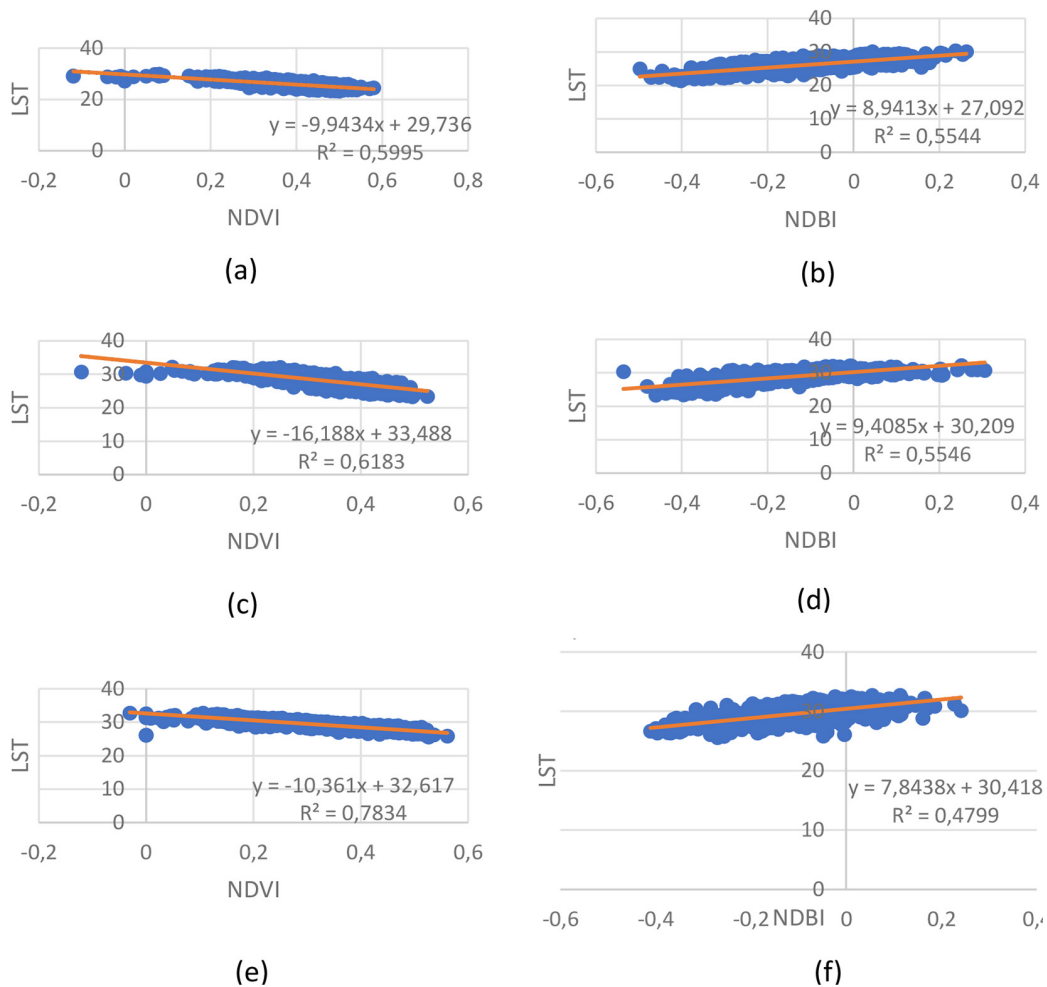


Figure 6. Correlation graphs of LST with NDVI and NDBI for 2016 (a) and (b), 2019 (c) and (d), 2022 (e) and (f)

statistically significant moderate positive correlation between LST and NDVI. The NDBI indicates that the expansion of built-up areas is positively correlated with an elevation in LST values. This observation is derived from the data indicating that there has been an increase in LST over time. Specifically, the range of LST values for built-up areas has expanded from 28 to 32 in 2016 to 30 to 35 °C in 2019, encompassing an area of 3,517 ha or 16.9% of the total. Furthermore, in 2022, the LST range has extended from 32 to 39, covering an area of 4,086 ha or 19.64% of the total.

Bima City land cover classification in 2016, 2019, and 2022

The land cover classification of Bima City encompasses five distinct categories, namely vegetation, water bodies, built-up, agricultural, and open field. In 2016, Bima City exhibited a significant prevalence of open land, encompassing an expansive area of 8,750 ha, accounting for approximately 42.06% of the total land area. Additionally, vegetation covered a substantial portion of the city, occupying 8,628 ha or 41.47% of the land. The land utilization patterns in Bima City undergo annual fluctuations. Each year, there is a reduction in the land area of vegetation lands and water bodies. In 2019, there was a 3.34% expansion in the built-up area, amounting to 695.

Additionally, open field witnessed a growth of 3.64%, equivalent to 757 ha. In 2022, there was a decrease in open field area by -109 ha, representing a reduction of 0.52%. Conversely, there was an increase in built-up area by 667 ha, indicating a growth of 3.2% during the same period. The data in Figure 7 illustrates the changes in land cover

for vegetation, water bodies, and agricultural area between 2019 and 2022. It is observed that the vegetation cover experienced a decrease of 398 ha or 1.91% in 2019, followed by a further decrease of 159 ha or 0.76% in 2022. Similarly, the water bodies decreased by 17 ha or 0.08% in 2019 and 2022 and a subsequent decrease of 8 ha or 0.04% in 2022. Furthermore, the agricultural area decreased by 1,136 ha or 4.98% in 2019 and a subsequent decrease of 391 ha or 1.88% in 2022.

The most significant land conversion observed from 2016 to 2022 involved the transformation of agricultural, spanning an area of 1,428 ha or 6.86% of the total land area. This conversion resulted in the emergence of built-up and open field. The extent of urbanized land experienced a notable expansion during the timeframe spanning from 2016 to 2022. The observed increase in land area was achieved through the conversion of agricultural measuring 1,362 ha, representing 6.54% of the total area, and an additional 66 ha of open field. The conversion of vegetated and water bodies into open field resulted in a total area of 648 ha, representing approximately 3.12% of the overall land area. According to Setiawan and Rudiarto (2016), Bima City witnessed a decline in vegetation and rice fields, alongside a rise in the extent of built-up, during the period spanning from 1999 to 2014. According to Nisah (2022), the most significant land transformation observed in Bima City from 2015 to 2021 involved converting vegetated areas into built-up and open field.

Land surface temperature distribution and land cover class

The spatial distribution of land surface temperature in Bima City exhibits temporal

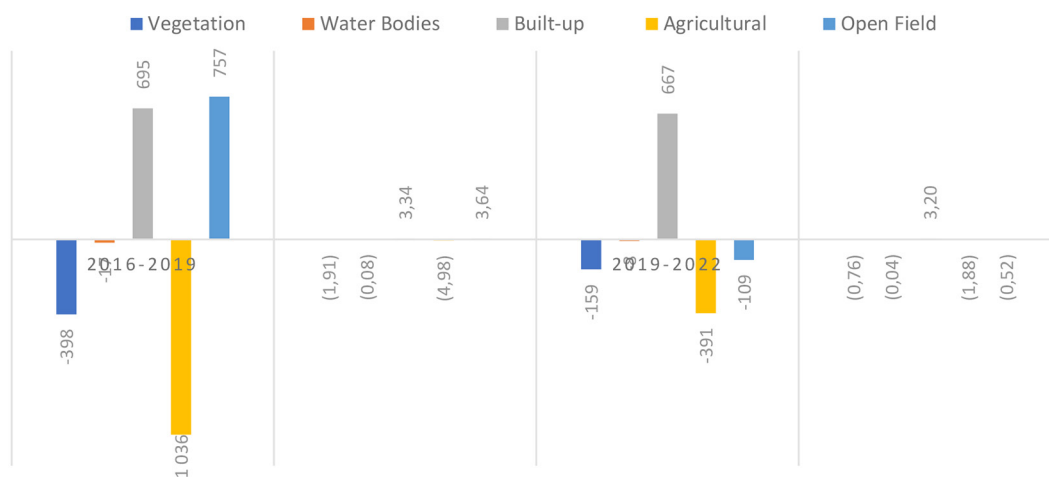


Figure 7. The changes in the area of Bima City land cover in 2016–2019 and 2019–2022

Table 4. The results of the land cover accuracy test for the city of Bima in 2016, 2019, and 2022

Overall accuracy (%)	Land cover				
	Vegetation	Water bodies	Built-up land	Agriculture	Open field
2016			95		
2019			93		
2022			94		

fluctuations in 2016, 2019, and 2022. According to an analysis of satellite data, the LST exhibited a range of approximately 20.50 °C to 32.54 °C in 2016, a range of approximately 20.72 °C to 35.08 °C in 2019, and a range of approximately 16.99 to 39.18 °C in 2022 (Figure 3, 4, and 5). This study examines the distribution of LST and the spatial extent and location of temperature changes within each land cover class in Bima City during the years 2016, 2019, and 2022. In 2016, the highest recorded temperature within the vegetation cover class reached 32.54 °C. The designated area measures 24.36 ha, accounting for 0.28% of the total land area. Additionally, the minimum temperature recorded in this area is 20.50 °C. Another portion of land, spanning 2,200 ha, represents 25.50% of the overall land area. The temperature distribution within the vegetation cover class was recorded as 8,628 ha, or 41.50% of the total. The minimum LST recorded is 20.50 °C, covering an area of 2,200.36 ha, which accounts for 25.52% of the total area.

In 2019, a notable rise was observed in the maximum temperature distribution within the vegetation land cover class, with an increase of 190.33 ha or 2.31%. This increase further escalated to 436.12 ha or 5.40% by 2022. The area of the vegetation cover class experienced a decrease in its minimum LST by 590.54 ha or 5.94% between 2019 and 2022. Additionally, there was a decrease of 287.46 ha or 3.18% in the same period. Between 2016, 2019, and 2022, there was an observed increase in open land cover by 648 ha, representing a growth rate of 3.15%.

Additionally, Figure 7 illustrates the conversion of 557 ha, or 9.12%, of vegetation into open field. The land cover of water bodies exhibited an increase in the maximum LST area of 1.18 ha or 4.88% between 2019 and 2022. Similarly, there was an increase in the minimum LST area of 1.03 ha or 5.56% during the same period. However, in 2022, there was a decrease in the minimum LST area by 0.08 ha or 0.14%.

The characteristic of LST in Bima City in 2016 correlated with the trajectory of urban

infrastructure development. Figure 3 illustrates LST distribution within the built-up cover class. The built-up cover class exhibits a maximum LST area of 717 ha, accounting for 71.81% of the total. In 2016, this land cover class had a building density value, as measured by the NDBI of 0.47. The minimum LST of an area measuring 3.68 ha or 0.37% of the total area. In 2019, there was a reduction in the maximum LST area by 165 ha, which accounted for a decrease of 39.25%.

Similarly, in 2022, there was a decrease of 100 ha, representing a decline of 13.48%. The observed phenomenon of a 6.86% increase in the built-up area resulting from the conversion of agricultural by 1,428 ha indicates a positive trend in the expansion of built-up and open field. Figure 7 illustrates the observed expansion of built-up area during the timeframe spanning from 2016 to 2022. During the time frame encompassing 2016, 2019, and 2022, there was a reduction in the maximum LST area of the agricultural land cover class by 223.10 ha, representing a decrease of 8.95%. Additionally, in 2019 and 2022, there was a decrease in the minimum area of LST by 6.35 ha, equivalent to a decline of 1.10%. Conversely, in 2022, there was an increase in the minimum area of LST by 29.99 ha, indicating a rise of 3.49%.

The open field category substantially increased its maximum LST between 2016 and 2022. The total area in question reached 1,747.72 ha equivalent to 17.45% of the total, in 2019 and 2022. This figure corresponds to 421.69 ha or 4.82% of the total. One contributing factor to this rise in the land area was converting vegetation, agricultural, and water bodies into open field, totalling 648 ha. This study aims to examine the process of expanding critical land in Bima City, as discussed by Nisah (2022). Fadlin et al. (2020) conducted a study. According to Senanayake et al. (2013) which use low albedo materials leading to high heat absorption in urban centres. In addition, removal of vegetation cover and emissions of waste heat from various sources contribute to the accumulation of heat energy, leading to formation of urban heat islands (UHIs, regions characterized by favourable environmental

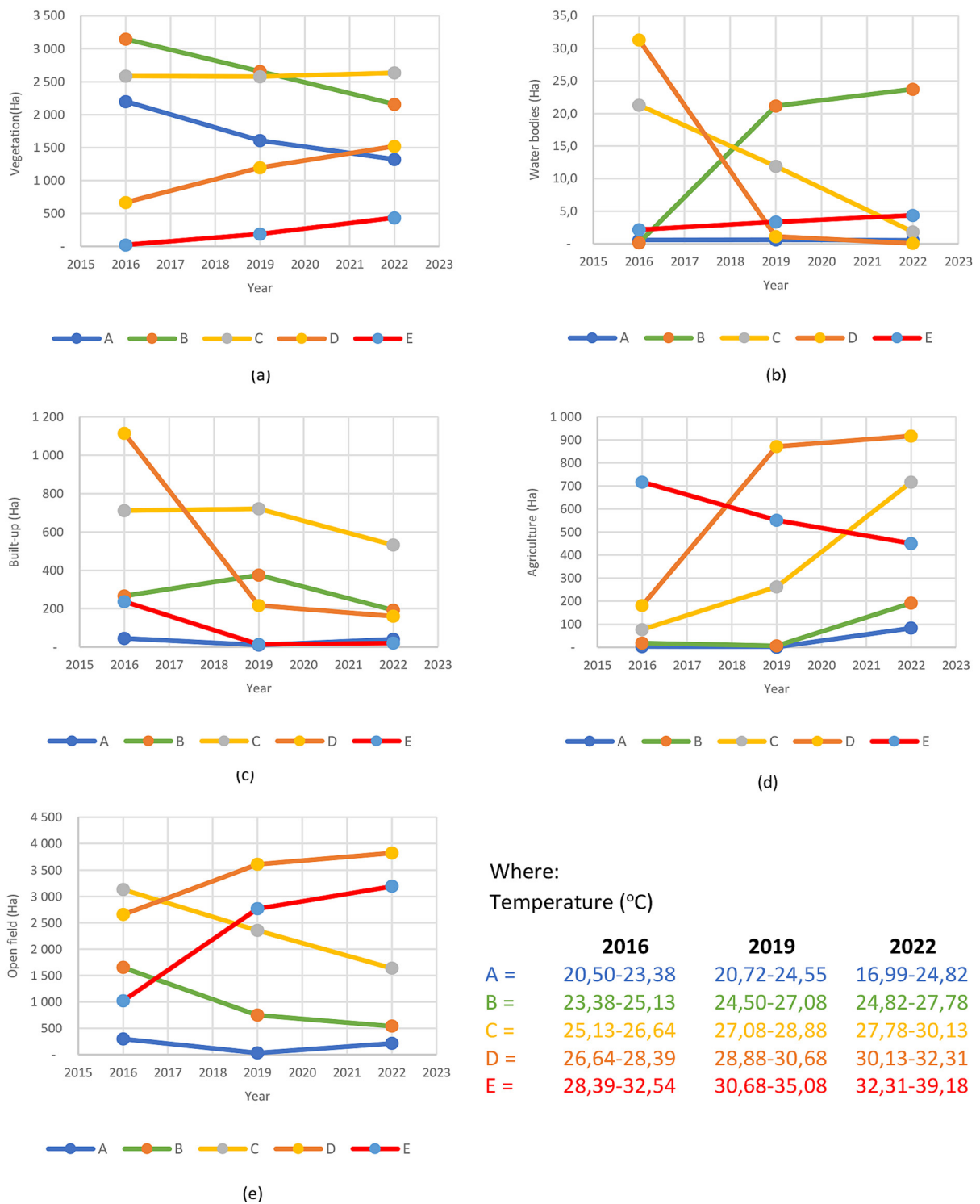


Figure 8. The changes in land surface temperature in the (a), (b), (c), (d), and (e) land cover class of Bima City in 2016, 2019 and 2022

conditions exhibit an elevation in Land Surface Temperature (LST) scores.

Urban heat island detection

The identification of urban heat island (UHI) presence in Bima City involves the utilization of equations (9), (10), and (11) to establish the air

temperature threshold for UHI occurrence. Additionally, UHI threshold calculations facilitate the spatial mapping of UHI phenomena distribution within Bima City. Furthermore, equation (12) is utilized for UHI Index analysis, enabling an assessment of the extent of UHI phenomenon potential. The UHI index is categorized into three distinct classes: non-UHI, potential UHI, and UHI.

Table 5. UHI threshold in 2016, 2019, and 2022

Year	T_{max}	T_{min}	$T_{men} (\mu)$	Standard deviation (σ)	UHI threshold $\mu + 0.5 \cdot \sigma$ ($^{\circ}\text{C}$)
2016	32.54	20.50	25.73	1.99	26.73
2019	35.08	20.50	28.35	2.44	29.57
2022	39.18	16.99	29.70	3.02	31.21

Bima City is a service-oriented urban centre, serving as the primary economic hub for the Bima Regency and Dompu Regency regions. It facilitates various community activities, including trade and education. The progression of Bima City over time necessitates acknowledging the inevitable occurrence of the urban heat island phenomenon in the area.

The analysis of the temperature threshold at which the UHI phenomenon occurs in Bima City indicates that the region is indeed experiencing the UHI effect. The determined threshold temperature for the UHI phenomenon 2016 was recorded as 26.73%. If the land surface temperature exceeds 26.73%, it signifies the presence of the urban heat island phenomenon in the respective area. The findings of the analysis of the urban heat island phenomenon in Bima City during the year 2016 are displayed in Table 6. According to the findings presented in Figure 10, the UHI

phenomenon exhibits a notable concentration within the city’s central region, subsequently extending to the surrounding areas.

The urban heat island phenomenon’s prevalence in Bima City is 9.57% of its total area. Additionally, 22.40% of the city’s area exhibits potential for experiencing the UHI phenomenon, while the remaining 68.03% of Bima City’s total area remains unaffected by the UHI phenomenon. The production of a map illustrating the distribution of UHI phenomena in Bima City in 2016 can be facilitated by utilising the UHI index, as depicted in Figures 9 and 10. Regions with land LST exceeding 29.57 indicate UHI areas, whereas regions with LST ranging from 0.0 $^{\circ}\text{C}$ to 29.57 $^{\circ}\text{C}$ indicate non-UHI regions. The UHI conditions in Bima City during the year 2019 were examined (Table 7).

The UHI phenomenon’s prevalence in Bima City is 9.57% of its total area. Additionally, 22.40% of the city’s area exhibits potential for

Table 6. The UHI phenomenon in Bima City based on LST in 2016

Class land surface temperature ($^{\circ}\text{C}$)	UHI class	Index UHI	Area (ha)	Percentage (%)
20.50–23.38	Non UHI	-4.79	14,153.29	68.03
23.38–25.13		-2.47		
25.13–26.64		-0.84		
26.64–28.39	UHI potential	0.91	4,659.95	22.40
28.39–32.54	UHI	3.87	1,991.76	9.57
Total			20,805.00	100.00

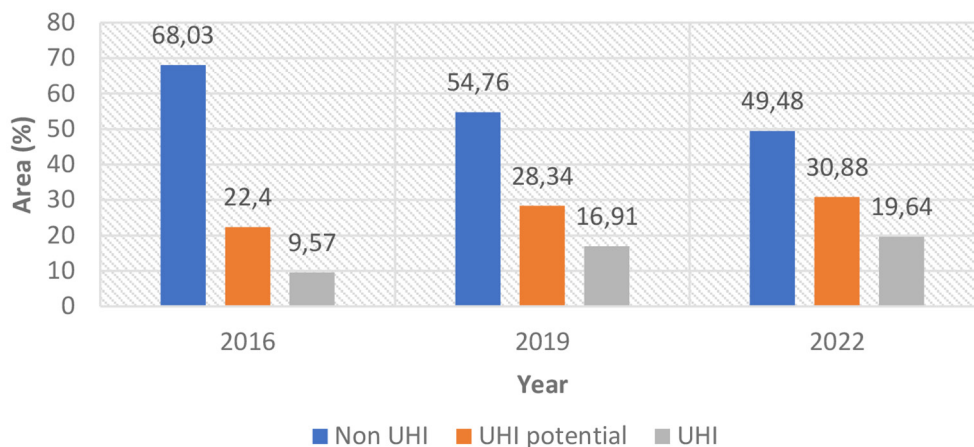


Figure 9. The comparison of UHI condition in Bima city for 2016, 2019, and 2022

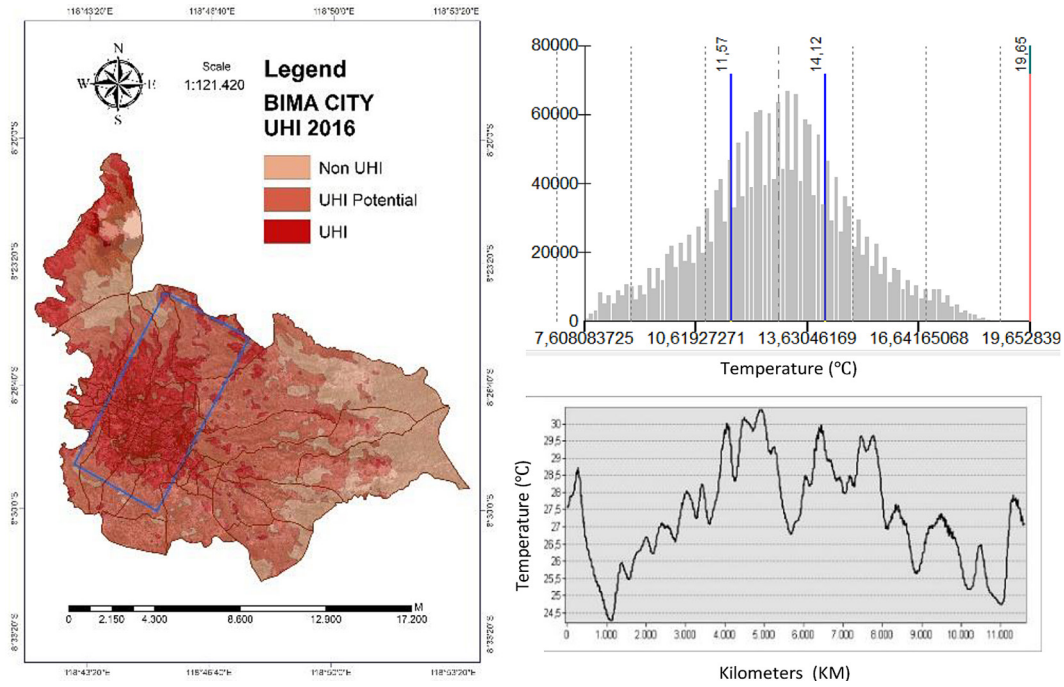


Figure 10. The urban heat island in Bima city for 2016

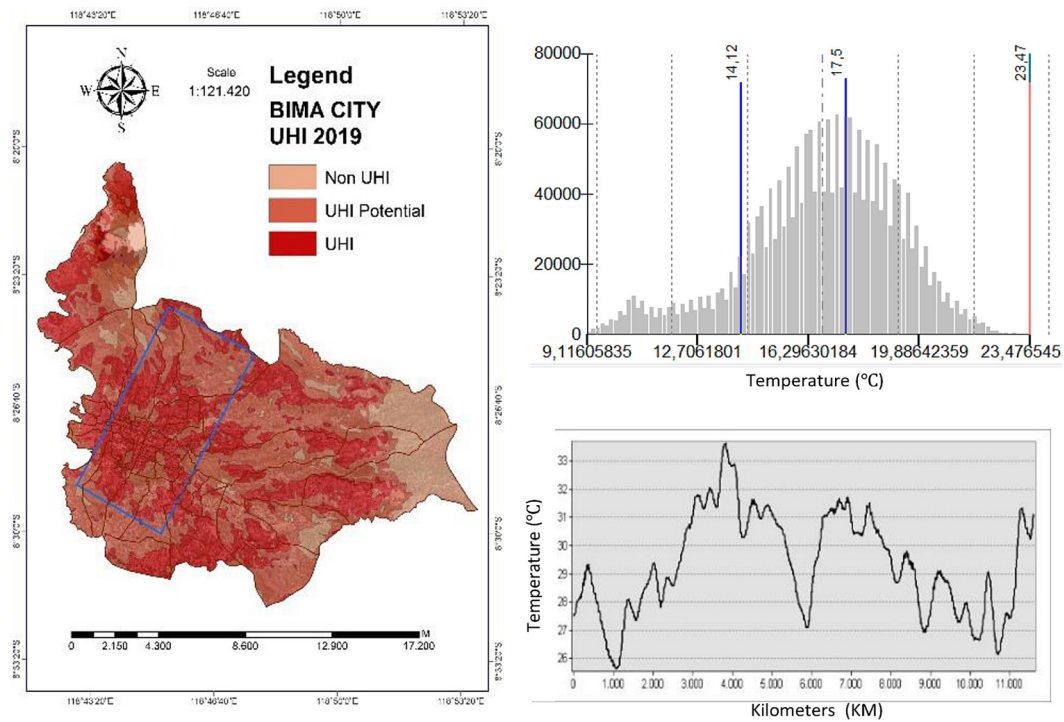


Figure 11. The urban heat island in Bima city for 2019

Table 7. The UHI phenomenon in Bima City Based on LST in 2019

Class land surface temperature (°C)	UHI class	Index UHI	Area (ha)	Percentage (%)
20.72–24.55	Non UHI	-6.94	11,392.72	54.76
24.55–27.08		-3.76		
27.08–28.88		-1.59		
28.88–30.68	UHI potential	0.21	5,895.17	28.34
30.68–35.08	UHI	3.31	3,517.12	16.91
Total			20,805.00	100.00

Table 8. The UHI phenomenon in Bima City based on LST in 2022

Class land surface temperature (°C)	UHI class	Index UHI	Area (ha)	Percentage (%)
16.99–24.82	Non UHI	-10.31	10,294.27	49.48
24.82–27.78		-4.91		
27.78–30.13		-2.26		
30.13–32.31	UHI potential	0.01	6,424.60	30.88
32.31–39.18	UHI	4.54		19.64
Total			20,805.00	100.00

experiencing the UHI phenomenon, while the remaining 68.03% of Bima City’s total area remains unaffected by the UHI phenomenon. The production of a map illustrating the distribution of UHI phenomena in Bima City in 2016 can be facilitated by utilising the UHI Index, as depicted in Figures 9 and 10. Regions with LST exceeding 29.57 °C indicate UHI areas, whereas regions with LST ranging from 0.0 °C to 29.57 °C indicate non-UHI regions. The UHI conditions in Bima City during the year 2019 were examined by employing the UHI index.

The UHI conditions in Bima City experienced a temperature increase of 31.21 °C in 2022. The UHI category refers to a specific geographical region with a UHI index of 4.54 °C. This region spans an area of 4,086 ha, which accounts for approximately 19.64% of the total area of Bima City. Table 8 presents the UHI phenomenon observed in Bima City. Figure 12 depicts the spatial

distribution of the UHI phenomenon in Bima City in the year 2022 is depicted. Based on the analysis, it is evident that the UHI phenomenon exhibits a comparable pattern to that of the preceding year, disseminating across the adjacent region.

Environmental sustainability governance LST in Bima City was evaluated by analyzing surface temperature data obtained from Landsat 8 (OLI/TIRS) imagery for the years 2016, 2019, and 2022. The data was sourced from the Google Earth Engine data portal. The data indicate that Bima City witnessed a rise in the UHI coverage from 9.57% in 2016 to 16.91% in 2019 and further to 19.64% in 2022, relative to the total area of the city affected by this phenomenon. Figure 9 illustrates the comparative graph of the UHI region in Bima City for 2016, 2019, and 2022.

Potential strategies stakeholders in Bima City can implement to mitigate the effects of UHI. Effective vegetation management in land

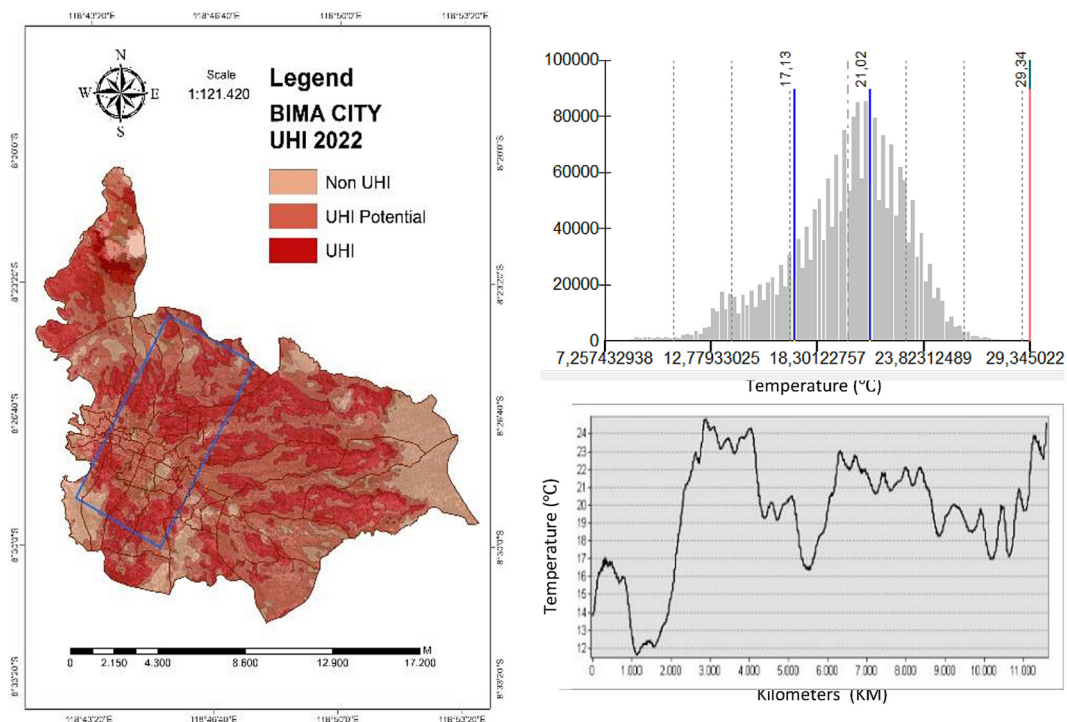


Figure 12. The urban heat island in Bima city for 2022

development is crucial for establishing a favourable microclimate that promotes coolness and health in urban regions. There is a need to enhance the control system to use urban space more ecologically sustainably. This can be achieved by augmenting the presence of green open spaces within the city's vicinity and incorporating elements into government infrastructure and residential building environments. It is imperative to develop comprehensive regulatory frameworks for green infrastructure buildings. To ensure the successful implementation of development control, it is crucial to adhere to designated land use, employ appropriate building materials and construction techniques, and establish sustainable urban space infrastructure. Additional investigation is warranted to explore the impact of urban built-up land cover configuration on escalating the UHI phenomenon. Czubaszek and Wysocka-Czubaszek (2016) found that the presence of vegetation and water bodies in the land cover class notably reduces the UHI effect.

CONCLUSIONS

The study's findings indicate that the UHI phenomenon in Bima City encompassed approximately 31.97% of the total land area in 2016. The areas with potential UHI occurrence accounted for 31.34% of the total area, while the remaining 36.69% did not exhibit UHI characteristics. The recorded threshold temperature for the UHI phenomenon in Bima City was 26.73 °C. Additional findings indicate that the dominance of UHI in 2016 was primarily observed in areas with pre-existing land cover. In 2019, there was a notable rise in UHI coverage, encompassing approximately 45.26% of all regions. Among these regions, 28.48% exhibited potential for UHI development, while 26.26% remained unaffected by UHI. The threshold temperature for UHI was measured to be 29.57 °C. This indicates that the UHI phenomenon was prevalent in Bima City, particularly in areas with high built-up land cover and open field. In 2022, the UHI phenomenon experienced a notable rise, reaching 50.52%. This increase was particularly prominent in regions characterized by open land cover, with an estimated coverage of 26.51%. In contrast, non-UHI areas accounted for 22.98% of the total, while the threshold temperature for UHI was determined to be 31.21 °C.

REFERENCES

1. Ahmed S. 2018. Assessment of urban heat islands and impact of climate change on socioeconomic over Suez Governorate using remote sensing and GIS techniques. *Egypt J Remote Sens Sp Sci.*, 21(1), 15–25. doi: 10.1016/j.ejrs.2017.08.001.
2. Akher S., Chattopadhyay D.S. 2017. Impact of urbanization on land surface temperature – A case study of Kolkata New Town. *Int J Eng Sci.*, 6(1), 71–81. doi: 10.9790/1813-0601027181.
3. Alavipanah S., Schreyer J., Haase D., Lakes T., Qureshi S. 2018. The effect of multi-dimensional indicators on urban thermal conditions. *J Clean Prod.*, 177, 115–123. doi: 10.1016/j.jclepro.2017.12.187.
4. Athukorala D., Murayama Y. 2021. Urban heat island formation in greater Cairo: Spatio-temporal analysis of daytime and nighttime land surface temperatures along the urban-rural gradient. *Remote Sens.*, 13(7). doi: 10.3390/rs13071396.
5. Czubaszek R., Wysocka-Czubaszek A. 2016. Urban heat island in bialystok. *J Ecol Eng.*, 17(3), 60–65. doi: 10.12911/22998993/63323.
6. DKPS. 2016. Aggregate population of Bima City in 2016. (In Indonesian)
7. DKPS. 2022. Aggregate population of Bima City in 2022. (In Indonesian)
8. EEA. 2017. Climate change, impacts and vulnerability in Europe 2016. <https://www.eea.europa.eu/publications/climate-change-adaptation-and-disaster>.
9. El-Hattab M., Amany S.M., Lamia G.E. 2018. Monitoring and assessment of urban heat islands over the Southern region of Cairo Governorate, Egypt. *Egypt J Remote Sens Sp Sci.*, 21(3), 311–323. doi: 10.1016/j.ejrs.2017.08.008.
10. Fadlin F., Suparjo, Sajiah A.M., Ransi N., Nangi J. 2020. Spatiotemporal analysis of environmental criticality index using land surface temperature and normalized difference vegetation index Algorithms in Makassar City. (In Indonesian) *SemanTIK*, 6(1), 89–98.
11. Fawzi N.I. 2017. Measuring urban heat island using remote sensing, case of Yogyakarta City. *Maj Ilm Globe*, 19(2), 195–206.
12. Garouani M.E., Amyay M., Lahrach A., Oulidi H.J. 2021. Land surface temperature in response to land use/cover change based on remote sensing data and GIS techniques: Application to Saïss Plain, Morocco. *J Ecol Eng.*, 22(7), 100–112. doi: 10.12911/22998993/139065.
13. Ismoyojati G., Sujono J., Jayadi R., Teknik D., Teknik F., Gadjah U. 2019. Study of the effect of changes in land use on the flood characteristics of Bima City. February. (In Indonesian) doi: 10.7454/jglitrop.v2i2.46.

14. Jimenez-Munoz J.C., Sobrino J.A., Skokovic D., Mattar C., Cristobal J. 2014. Land surface temperature retrieval methods from landsat-8 thermal infrared sensor data. *IEEE Geosci Remote Sens Lett.*, 11(10), 1840–1843. doi: 10.1109/LGRS.2014.2312032.
15. Kamboj S., Ali S. 2020. Urban sprawl of Kota city: A case study of urban heat island linked with electric consumption. *Mater Today Proc.*, 46(40), 5304–5314. doi: 10.1016/j.matpr.2020.08.783.
16. Kaplan G., Avdan U., Avdan Z.Y. 2018. Urban Heat Island Analysis Using the Landsat 8 Satellite Data: A Case Study in Skopje, Macedonia.
17. Khoshnoodmotlagh S., Daneshi A., Gharari S., Verrelst J., Mirzaei M., Omrani H. 2021. Urban morphology detection and its linking with land surface temperature: A case study for Tehran Metropolis, Iran. *Sustain Cities Soc.* 74 October 2020:103228. doi: 10.1016/j.scs.2021.103228.
18. Kondo K., Mabon L., Bi Y., Chen Y., Hayabuchi Y. 2021. Balancing conflicting mitigation and adaptation behaviours of urban residents under climate change and the urban heat island effect. *Sustain Cities Soc.*, 65, 102585. doi: 10.1016/j.scs.2020.102585.
19. NISAH IU. 2022. Environmental criticality analysis based on environmental criticality index and urban heat island phenomenon in Bima City. (In Indonesian)
20. Nuruzzaman M. 2015. Urban heat island: causes, effects and mitigation measures – A review. *Int J Environ Monit Anal.*, 3(2), 67. doi: 10.11648/j.ijema.20150302.15.
21. Sejati A.W., Buchori I., Rudiarto I. 2019. The spatio-temporal trends of urban growth and surface urban heat islands over two decades in the Semarang Metropolitan Region. *Sustain Cities Soc.*, 46(2018), 101432. doi: 10.1016/j.scs.2019.101432.
22. Senanayake I.P., Welivitiya W.D.D.P., Nadeeka P.M. 2013. Remote sensing based analysis of urban heat islands with vegetation cover in Colombo city, Sri Lanka using Landsat-7 ETM+ data. *Urban Clim.*, 5, 19–35. doi: 10.1016/j.uclim.2013.07.004.
23. Setiawan B., Rudiarto I. 2016. Study of changes in land use and spatial structure of the City of Bima. (In Indonesian) *J Pembang Wil Kota.*, 11(4), 154. doi: 10.14710/pwk.v12i2.12892.
24. Tawfeeq Najah F., Fakhri Khalaf Abdullah S., Ameen Abdulkareem T. 2023. Urban land use changes: effect of green urban spaces transformation on urban heat islands in Baghdad. *Alexandria Eng J.*, 66, 555–571. doi: 10.1016/j.aej.2022.11.005.
25. U.S. Geological Survey. 2019. Landsat 8 Data Users Handbook. Volume ke-8. <https://landsat.usgs.gov/documents/Landsat8DataUsersHandbook.pdf>.
26. UNEP, 2022. Global Status Report for Buildings and Constr Uction. <https://globalabc.org/resources/publications/2022-global-status-report-buildings-and-construction>.
27. WHO Regional Office for Europe. 2017. Protecting Health in Europe from Climate Change: 2017 Update. <http://www.euro.who.int/pubrequest>.
28. Yang C., Yan F., Zhang S. 2020. Comparison of land surface and air temperatures for quantifying summer and winter urban heat island in a snow climate city. *J Environ Manage.*, 265(March), 110563. doi: 10.1016/j.jenvman.2020.110563.